Solid Freeform Fabrication 2017: Proceedings of the 28th Annual International Solid Freeform Fabrication Symposium – An Additive Manufacturing Conference
Reviewed Paper

POWDER BED FUSION METROLOGY FOR ADDITIVE MANUFACTURING DESIGN GUIDANCE

Jared Allison[1], Conner Sharpe[1], Carolyn Conner Seepersad[1], and Steven Kubiak[2]

[1]The University of Texas at Austin, Austin TX, 78712
[2]Stratasys Direct Manufacturing, Austin, TX, 78758

Abstract

Design for additive manufacturing (DFAM) guidelines are important for helping designers avoid iterations and fully leverage the design freedoms afforded by additive manufacturing (AM). Guidelines can be generated via metrology studies that use test parts to characterize statistically the geometric capabilities of specific AM processes. Towards that end, a test part is designed for polymer selective laser sintering (SLS) that incorporates an array of geometric features in an extremely compact volume, such that it can be easily inserted into existing builds. The part is then built in multiple materials, build orientations, and locations within the build chamber in a factorial-style study to assess the variation attributed to each processing parameter. Both part resolution and accuracy are investigated. Upon measurement of the test parts, tolerances and design allowables are established and compiled into a set of design guidelines for SLS. The guidelines are then made publicly accessible through an online web tool to be used by designers creating parts for polymer SLS.

Introduction

The focus of this study is to characterize the geometric capabilities of polymer SLS using a test part that is both compact and comprehensive. The test part, shown in Figure 1, includes five panels connected to a common base. The panels contain different features of interest to a designer and are detached from the base to be measured independently. The as-built dimensions of the test part form a cube measuring two inches along each side. By taking advantage of the self-supporting nature of the SLS powder bed, a high feature density is achieved by closely grouping the features.

By combining features found in previous test parts but arranging them in a nested form, this design features a comprehensive variety of features in a compact cube. The part is built as a single unit, similar to the parts proposed by Mahesh et al., Castillo, and Moylan et al. [1] [2] [3], but the detachable panels make it easy to access and measure each feature. The detachable panels are analogous to a suite of test parts used in the Govett et al. study [4], which utilized a separate test part for each type of feature, but in a much more compact form. Unlike some previous efforts that focus on characterizing the mechanical properties of SLS parts (e.g., [5]), this test part focuses exclusively on the geometric properties of SLS parts.

Although some previous studies have aimed to develop design guidelines that are independent of the specific AM process (e.g., [6]), process-specific investigations may be required to establish a more complete understanding of a particular AM process. Accordingly, the test part is designed specifically for the SLS process, which enables fabrication of all of the features. Even complex features such as the thin rods and hinges, as well as the nested configuration of panels, can be successfully built regardless of build orientation. The part could not be built in various orientations with a material extrusion process (e.g. FDM) without extensive support structures.

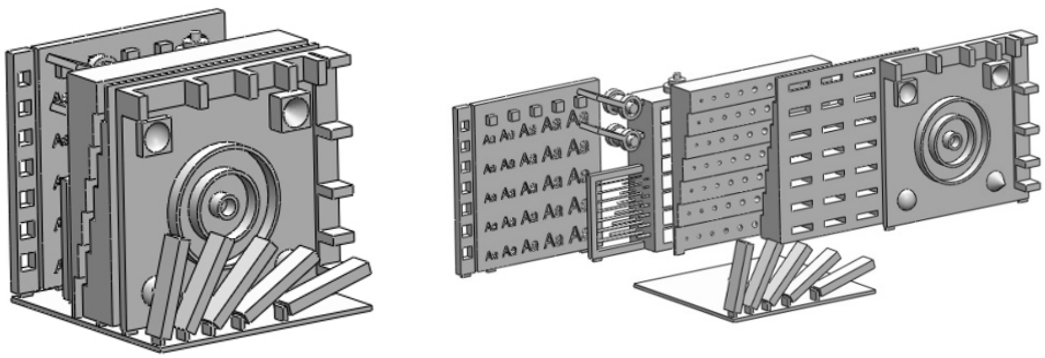

Figure 1: Polymer test cube as-built (left) and disassembled (right) [7]

The test cube features and feature sizes are shown in Table 1. Based on the results of the Govett et al. study, some feature sizes are selected such that they range from sizes that are too small to be resolved to sizes that are large enough to be resolved [4]. This range allows the resolution of the process to be identified.

Table 1: Polymer test cube feature ranges [7]

Feature	Feature Ranges	Incremement
Holes	0.8-2.60mm diameter	0.2mm
	1.0-10.0mm wall thickness	1.5mm
Thin rods	0.3-0.9mm diameter	0.1mm
Thin walls	0.2-0.8mm	0.1mm
Gaps	1.4-2.0mm gaps	0.2mm
	1.0-10.0mm wall thickness	1.5mm
Cylinders	2.0-8.0mm diameter	3.0mm
Hollow cylinders	5.0-25mm diameter	10.0mm
Domes	6.0mm diameter	-
Cones	6.0mm diameter 5.2mm height	-
Linear accuracy	5.0-12.5mm	2.5mm
Surface roughness	0°-90°	15°
Hinges	0.6mm and 1.0mm shaft clearances	-
Lettering	10-18pt font	2pt
	0.5-2.5mm emboss/raised depth	0.5mm
Snap Fits	-0.5-0.25mm offsets	0.05mm

As a means of comparison, the features included in previous test parts have been tabulated below along with the size of each part. The number of instances of each particular feature incorporated into the test part is shown in parentheses beside the feature description. Feature density is then calculated by dividing the total number of instances by the bounding volume of the part. Here it can be seen that the proposed part in this study not only occupies the smallest build volume, but also has the highest feature density. Feature density is a measure of the compactness of the test part. The high feature density of the proposed test part means that it can easily be placed into SLS builds without sacrificing the number of features investigated.

Table 2: Comparison of different test parts, including dimensions and feature density [7]

	Mahesh (2004)		Castillo (2005)		Govett (2012)		Moylan (2014)		Proposed Part	
Bounding Dimensions	170x170x20mm		60x81x100mm		-		~100x100x17mm		51x51x51mm	
Bounding Volume	578 cm^3		486 cm^3		~5,000 cm^3		~170 cm^3		131 cm^3	
Features Considered (Number of instances)	Holes	**(14)**	Holes	**(15)**	Holes	**(147)**	Holes	**(10)**	Holes	**(63)**
	Thin rods	**(6)**	Thin rods	**(5)**	Thin rods	**(15)**	Thin rods	**(5)**	Thin rods	**(21)**
	Thin walls	**(2)**	Thin walls	**(3)**	Thin walls	**(92)**	Cylinders	**(16)**	Thin walls	**(7)**
	Gaps	**(22)**	Domes	**(2)**	Gaps	**(154)**	Linear accuracy	**(10)**	Gap	**(28)**
	Hollow Cylinders	**(2)**	Square rods	**(5)**	Hole proximity to wall	**(73)**	Rectangular boss	**(10)**	Cylinders	**(3)**
	Domes	**(4)**	Bridge	**(1)**	Shaft clearance	**(104)**	Surface roughness	**(1)**	Hollow cylinders	**(3)**
	Cones	**(2)**	Warpage	**(1)**	Lettering	**(608)**	Flatness	**(1)**	Domes	**(2)**
	Square rods	**(8)**	Overhang angles	**(7)**	Gears	**(6)**	Build axis alignment	**(1)**	Cones	**(2)**
	Bridge	**(2)**					Lateral features of varied cross-section	**(8)**	Linear accuracy	**(8)**
	Hollow squares	**(2)**							Surface roughness	**(7)**
	Flatness	**(1)**							Hinges	**(2)**
	Straightness	**(1)**							Lettering	**(50)**
	Brackets	**(4)**							Snap Fits	**(5)**
Feature Density (instances/cm^3)		**0.12**		**0.08**		**0.24**		**0.36**		**1.53**

Experiment Design

The test part can be used in a factorial-style study to characterize the resolution and accuracy of SLS parts under a variety of conditions. Although a wide variety of process parameters can affect the resolution and accuracy of features, four specific factors are selected because they are often specified by the designer. The four factors are material choice, orientation of the test part within the build chamber, location of the test part within the build chamber, and machine identity [8] [9] [10] [11] [12] [13] [14]. By varying each of these factors, a factorial experiment can be conducted. Three different materials are considered: “neat” nylon 12 blend (PA 12), nylon 12 reinforced with glass beads (GF PA 12), and fire retardant nylon 11 (FR PA 11). The test cube is built in three different orientations, denoted by the plane of the build chamber in which the base is aligned: XY, XZ, and YZ. Location within the build chamber is reduced to two specifications: interior (I) where the cube is built in the center of the chamber and exterior (E) where the cube is built along the edges. Here, exterior is defined as the region bounded by the perimeter of the build area and a second perimeter that is offset from the first by two inches.

For a statistical characterization of polymer PBF, several copies of the test part must be built at each point in the experimental design. For each unique material, orientation, and location combination, five replicates are built on one machine, and three replicates on a second machine in order to assess the variability between PBF machines. In total, 144 test parts are required for the characterization.

All test parts are built by Stratasys Direct Manufacturing on 3D Systems Sinterstation 2500 Plus and 3D Systems Sinterstation HiQ+HS machines featuring Integra multizone heater upgrades. The build parameters are based on the 3D Systems default settings, but have been modified by Stratasys Direct Manufacturing in an effort to produce high quality, production parts. Nominally, the layer thickness and fill laser power are 100μm and 42W, respectively. After the build process, the parts are cleaned by Stratasys technicians using a combination of compressed air bead blasting and brush-like tools to remove any residual powder. The machines are maintained by Stratasys and tuned to production level specifications. Each of the test parts are inserted one-at-a-time into production builds.

Results

The measurement results are compiled into a set of guidelines that can be used by designers creating parts for polymer SLS. The guidelines are made available publicly through an online web tool that can be accessed at http://designforam.me.utexas.edu/. A screenshot from the tool is shown in Figure 2. The web tool contains all measurement results as well as a description of the measurement procedure. The web tool provides a detailed account of the specific effects attributed to each of the parameters in the study. Presented here are the average results from the 144 test cubes in the experimental design.

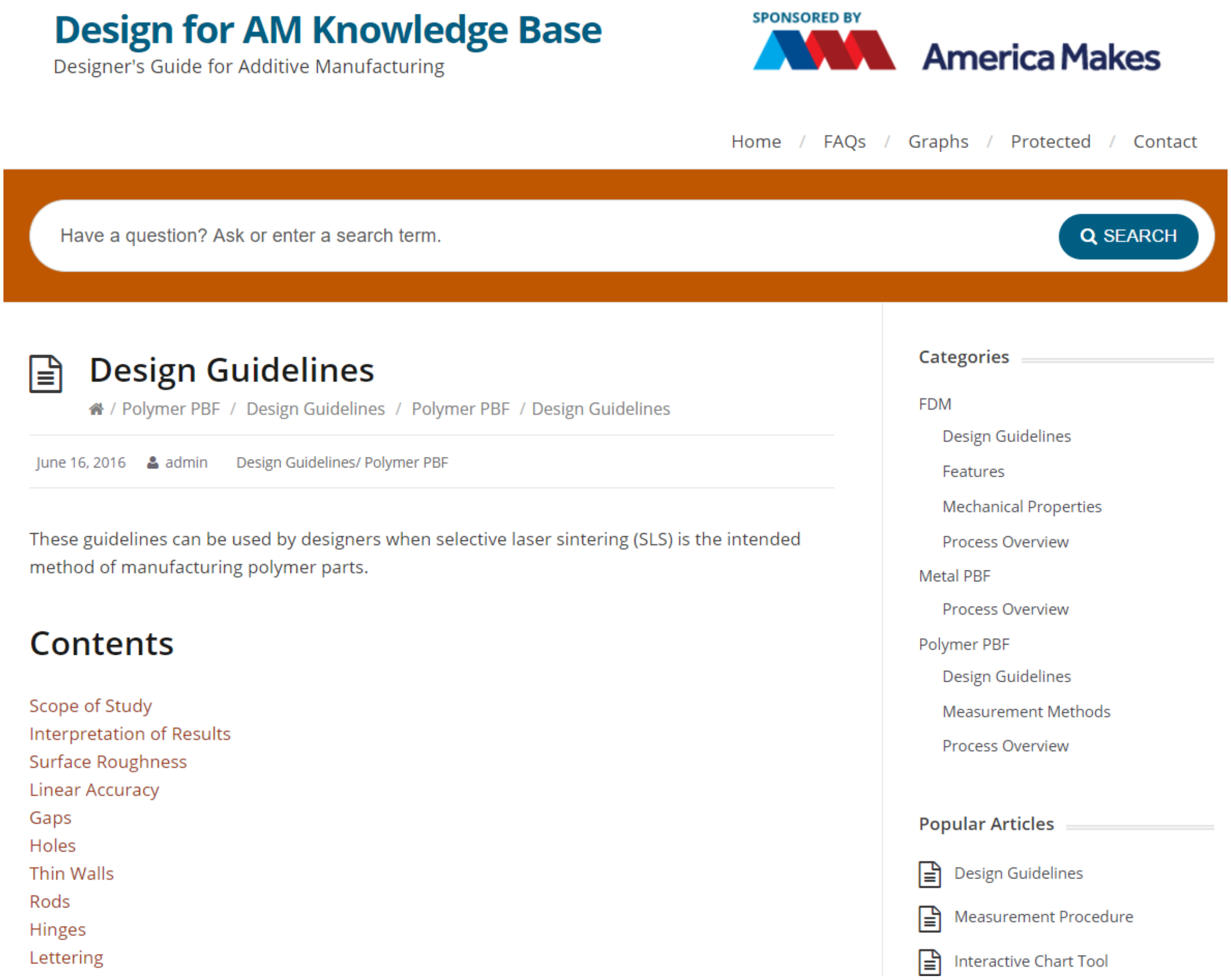

Figure 2: Online web tool layout

Surface Roughness

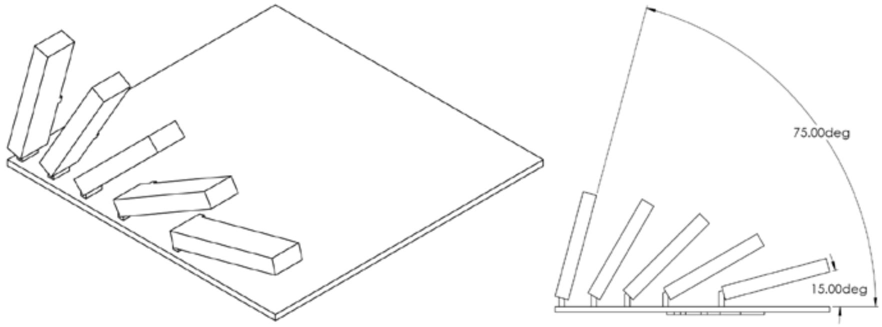

Figure 3: Surface roughness features in the test part

The test part features used to evaluate the surface roughness at various build angles are shown in Figure 3. Surface roughness is measured using a Zeta 3D optical surface profiler (3.1mm by 1.2mm field of view). The average surface roughness results from all test cubes are shown in Figure 4. The surface roughness is smallest at an angle of zero degrees relative to the build plane. The maximum roughness occurs at 15 degrees then decreases at all subsequent angles. Despite the decreasing trend, the roughness still reaches its minimum value at zero degrees. FR PA 11 is rougher than both PA 12 and GF PA 12, which have similar values of roughness. There does not appear to be a strong correlation between location within the build chamber and surface roughness.

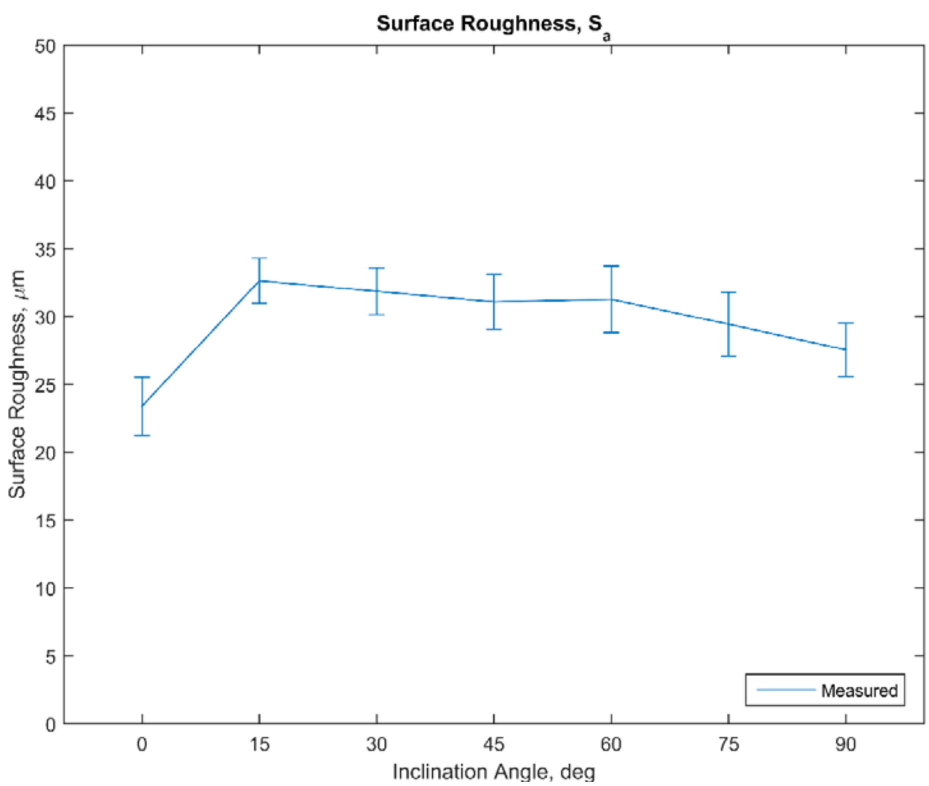

Figure 4: Average surface roughness as a function of build angle for all test cubes

Discussion

Surface roughness is smallest at zero degrees relative to the build plane and is largest at 15 degrees. This difference in roughness can be attributed to the stair-stepping effect between successive layers. As the angle is increased, the effect becomes less pronounced. Considering the materials used in the study, FR PA 11 has greater surface roughness than both PA 12 and GF PA 12. Location within the build chamber does not appear to impact surface roughness.

Linear Accuracy

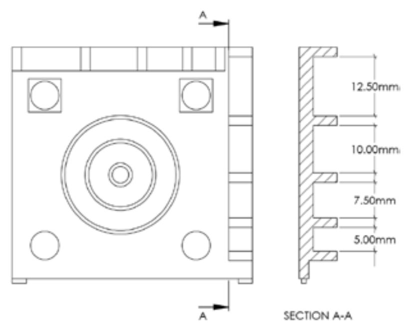

Figure 5: Linear accuracy features in the test part. Features of interest are tabs aligned along the outer edge of the part.

Linear accuracy indicates how well the machine is able to hold linear dimensions with respect to the prescribed dimensions within the CAD model. Linear accuracy in each build axis is determined by measuring the gap between successive walls. Figure 5 shows the linear accuracy features in the test part. The measurements are taken with iGaging digital calipers (0.01mm resolution).

Accuracy

The linear accuracy results are shown in Figure 6. SLS tends to undersize dimensions by approximately 0.2mm. When built, each of the measured distances in Figure 5 are generally 0.2mm smaller than their designed value. This trend appears to be independent of size and is consistent across the entire range of measurements.

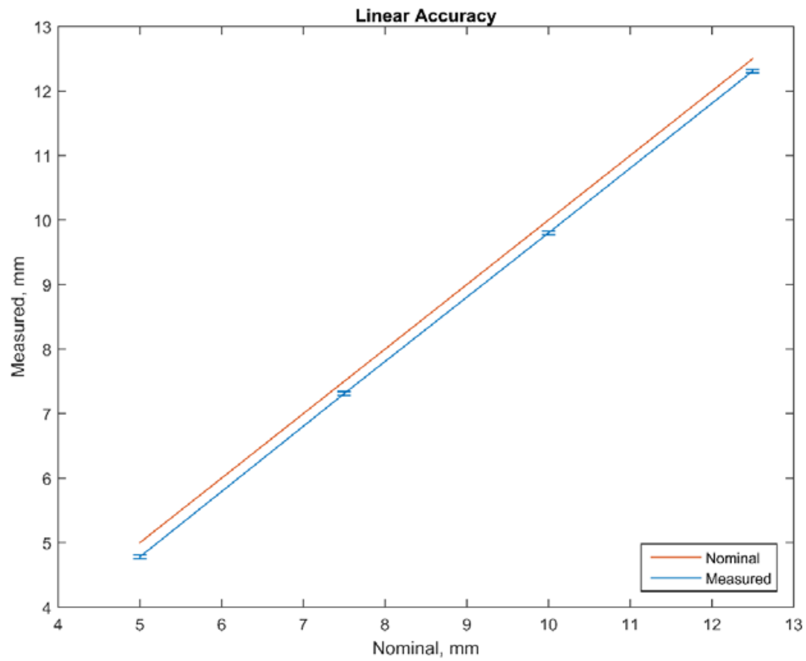

Figure 6: Linear accuracy trend for all test cube measurements. The red line indicates the nominal as-designed value, and the error bars correspond to 95% confidence intervals about the mean.

Discussion

Features built on the interior of the build chamber are usually more undersized than those built along the perimeter. With respect to orientation, distances along the Z axis of the build chamber tend to be closer to the defined CAD dimension than along the X or Y axes. PA 12 has the highest level of accuracy, followed by GF PA 12 and FR PA 11.

Gap Accuracy as a Function of Wall Thickness

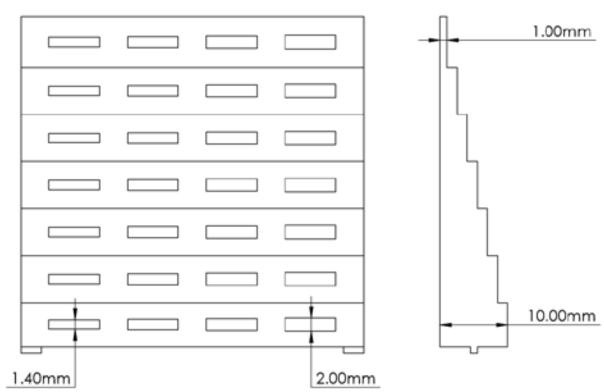

Figure 7: Features for evaluating gap accuracy as a function of wall thickness in the test part

Gap accuracy is determined by varying the gap size and the thickness of the wall through which the gap is created. The reported value corresponds to the gap measured along the axis of interest. Four gaps of varying dimensions are placed within each of the seven walls, as shown in Figure 7. Gap accuracy is measured using iGaging digital calipers (0.01mm resolution).

Accuracy

Similar to linear accuracy, gaps tend to be undersized by approximately 0.2mm. There does not appear to be a significant dependence on wall thickness.

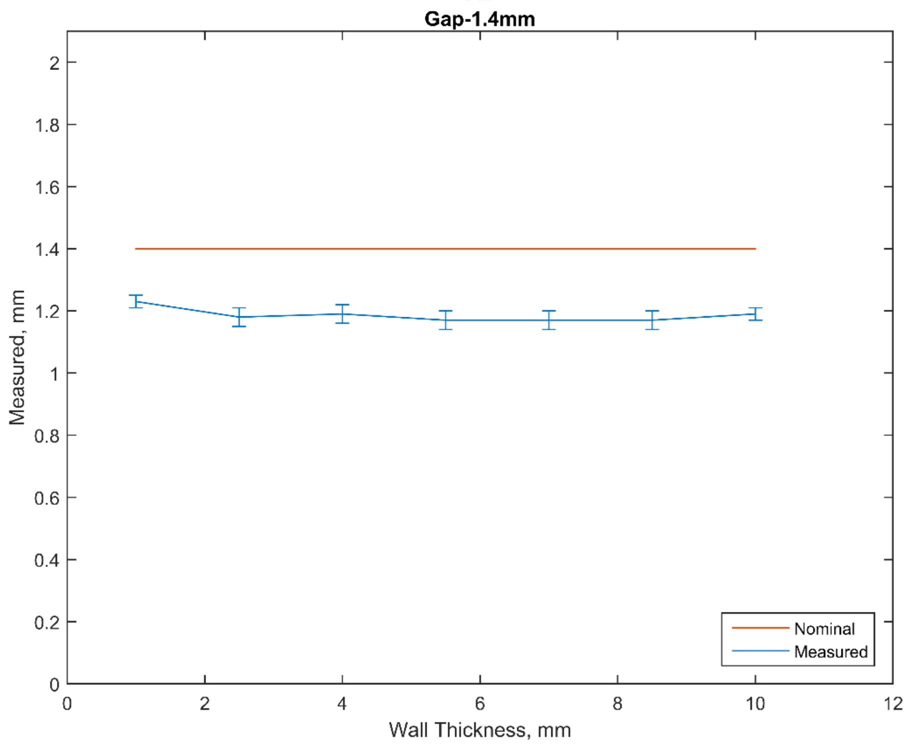

Figure 8: 1.4mm gap accuracy as a function of wall thickness for all test cubes. The red line indicates the nominal as-designed value, and the error bars correspond to 95% confidence intervals about the mean.

Discussion

Similar to linear accuracy, gaps aligned with the Z axis of the build chamber are generally the closest to the prescribed CAD dimensions. Additionally, PA 12 tends to be more accurate than both GF PA 1 2and FR PA 11. Location within the build chamber does not appear to significantly affect the accuracy of gaps.

Hole Diameter as a Function of Wall Thickness

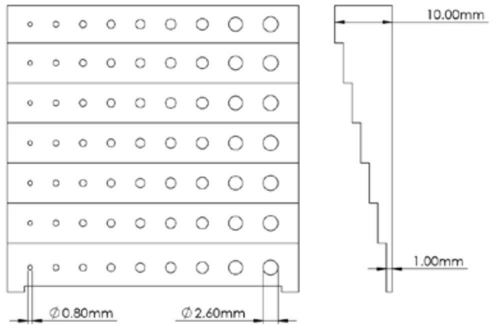

Figure 9: Features for evaluating hole accuracy and resolution as a function of wall thickness in the test part

Hole accuracy and resolution are determined by varying hole diameter as well as the thickness of the wall through which the hole is created. Hole resolution denotes the smallest hole that is reliably formed at each wall thickness. Accuracy provides quantitative comparisons of the mean hole diameter measured at each wall thickness to the as-designed diameter for the two largest holes (two rightmost columns of holes in Figure 9). Accuracy is measured using a flatbed scanner and digital image processing in Matlab. Hole resolution is determined through visual inspection.

Accuracy

Accuracy is measured for hole diameters of 2.4mm and 2.6mm across all wall thicknesses. Hole diameters have a tendency to be undersized by approximately 0.4mm, as shown in Figure 10. The trend does appear to depend on the thickness of the wall, with thicker walls yielding smaller holes than thinner walls.

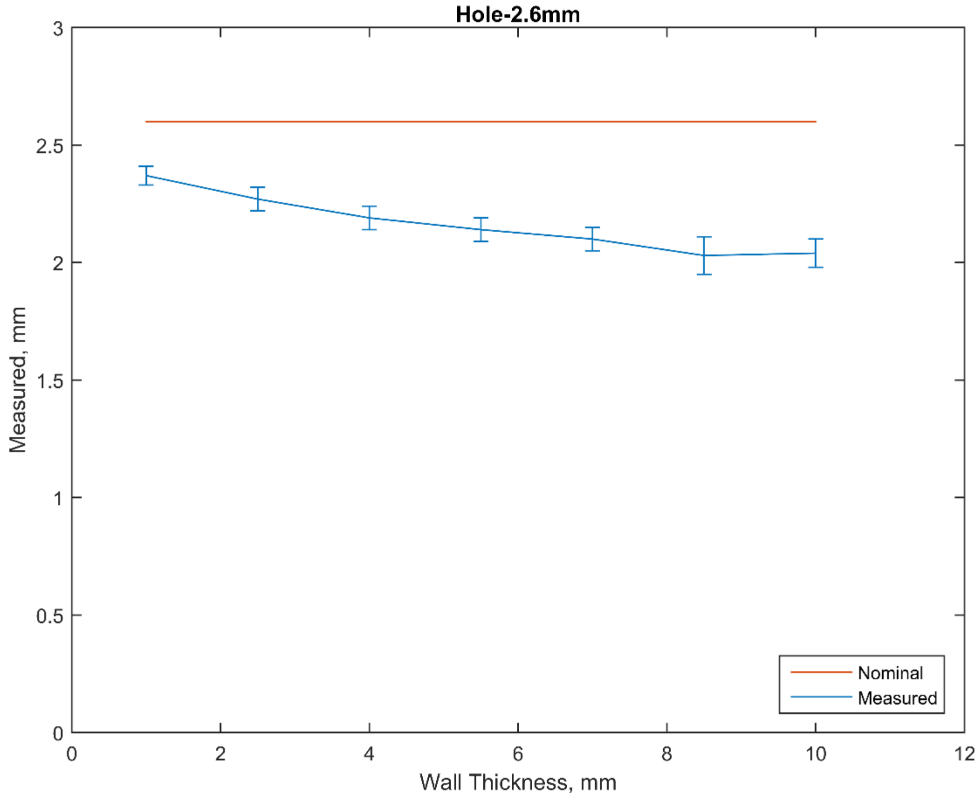

Figure 10: 2.6mm hole accuracy as a function of wall thickness for all test cubes. The red line indicates the nominal as-designed value, and the error bars correspond to 95% confidence intervals about the mean.

Resolution

Hole resolution appears to depend greatly on wall thickness. Thinner walls resolve smaller holes, and the smallest resolvable hole diameter tends to increase with wall thickness. In general, 1.0mm thick walls can reliably resolve (>75% of the time) 1.0mm holes. Conversely, 8.5mm thick walls can only resolve 2.0mm holes reliably.

Table 3: Hole diameter resolution as a function of wall thickness for all test cubes. The values within each cell indicate the proportion of observed instances that correctly resolved.

		Holes						
		Hole Diameter (mm)						
		2.0	1.8	1.6	1.4	1.2	1.0	0.8
Wall Thickness (mm)	1.0	0.96	0.95	0.94	0.92	0.85	0.76	0.69
	2.5	0.91	0.88	0.86	0.78	0.7	0.57	0.41
	4.0	0.83	0.8	0.69	0.6	0.49	0.35	0.23
	5.5	0.68	0.6	0.55	0.43	0.35	0.24	0.05
	7.0	0.58	0.51	0.43	0.36	0.22	0.13	0.04
	8.5	0.5	0.43	0.37	0.26	0.16	0.07	0.04
	10.0	0.5	0.4	0.32	0.17	0.08	0.06	0.04

Discussion

Holes tend to be the most undersized when the axis is orthogonal to the build chamber. As with the previous features, PA 12 produces holes that are the most accurate and are able to resolve the smallest holes. Location within the build chamber does not appear to influence the resolution or accuracy of holes.

Thin Walls

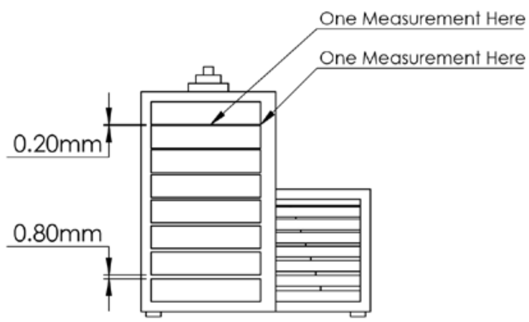

Figure 11: Thin wall features in the test part

Both accuracy and resolution are evaluated for thin walls. Two measurements are taken for thin walls – one at the base, and one at the middle – to assess the accuracy of wall thickness at different points along the wall. Figure 11 shows the thin wall features in the test part as well as the two locations in which measurements are taken. The accuracy of thin walls is measured using iGaging digital calipers (0.01mm resolution). Resolution is dictated by the thinnest wall that can be reliably built. Thin walls are built with thicknesses ranging from 0.2mm to 0.8mm in increments of 0.1mm.

Accuracy

Thin walls are usually oversized by approximately 0.2mm. This trend does not depend significantly on the thickness of the wall, but thicker walls are sometimes more oversized than thin walls.

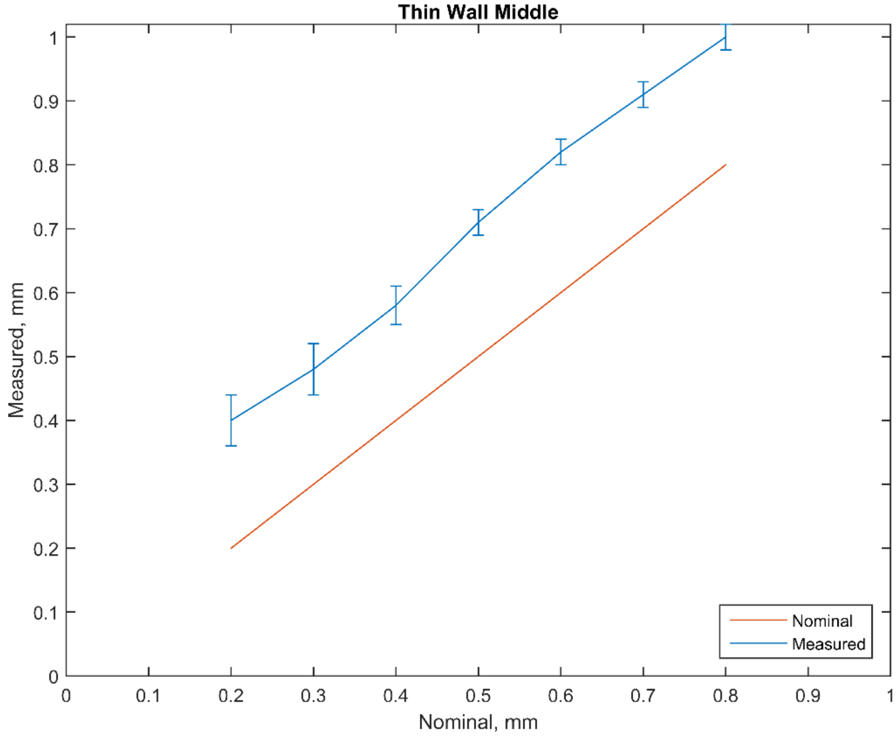

Figure 12: Thin wall accuracy for all test cubes. Measurements were taken in the middle of the wall. The red line indicates the nominal as-designed value, and the error bars correspond to 95% confidence intervals about the mean.

Resolution

In general, the thinnest resolvable walls are 0.5mm thick. All walls thicker than 0.6mm resolved successfully.

Table 4: Thin wall resolution for all test cubes. The values within each cell indicate the proportion of observed instances that correctly resolved.

Thin Walls	
Wall Thickness (mm)	Pass Proportion
0.2	0.34
0.3	0.39
0.4	0.49
0.5	0.92
0.6	1
0.7	1
0.8	1

Discussion

Thin walls are the most accurate when they are built parallel to the build chamber. This is due to the fact that SLS layers are 100µm thick while the spot size is typically 450µm in diameter. Again, PA 12 produces the most accurate walls; GF PA 12 and FR PA 11 have similar accuracy. Location within the build chamber does not usually affect thin wall accuracy. When the effect is observed, however, walls built in the interior portion of the build chamber are generally less oversized than in the exterior.

Thin Rods

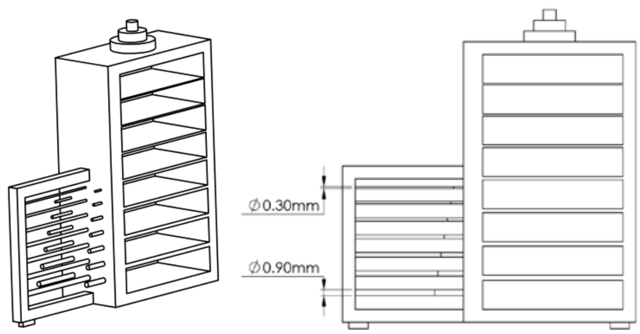

Figure 13: Thin rod features in the test part

Three types of rods are tested for resolution, and the test part is depicted in Figure 13. Supported rods are connected to side walls at both ends, while unsupported rods are cantilevered. Aspect ratios (length/diameter) of 5 and 10 are used for short and long unsupported rods, respectively, with rod diameters varying from 0.3mm to 0.9mm in 0.1mm increments. Thin rod resolution is evaluated through visual inspection.

Resolution

No significant relationship is observed between the support conditions and the ability to resolve thin rods. In order to ensure reliable resolution of thin rods, they should generally be at least 0.6mm in diameter. Smaller rods tend to fail or leave an “empty” spot in their place.

Table 5: Thin rod resolution for short (aspect ratio = 5), long (aspect ratio = 10), and fully supported. The values within each cell indicate the proportion of observed instances that correctly resolved.

		Short	Long	Supported
		Pass Proportion		
Rod Diameter (mm)	0.3	0.42	0.42	0.42
	0.4	0.35	0.35	0.34
	0.5	0.68	0.69	0.68
	0.6	0.97	0.97	0.96
	0.7	0.99	0.99	0.99
	0.8	0.99	0.99	0.99
	0.9	0.99	0.99	0.99

Discussion

Thin rods tend to have the best resolution when the primary axis is along the Z axis of the build chamber. For this orientation, the laser spot traces the cross section of the rod at each layer. It is worth noting that the diameter of the rods is not considered. Concerning material choice, GF PA 12 resolves thin rods better than the other two materials. This is a different result from the previous features. Thin rod resolution does not depend on location within the build chamber.

Hinges

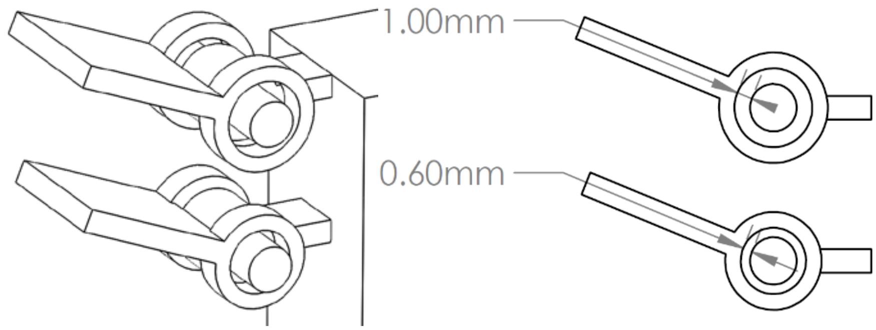

Figure 14: Hinge features in the test part

Two hinge designs are tested by varying the gap between the shaft of the hinge and the knuckle. Figure 14 shows the two designs. The hinges are tested by checking whether they can move freely, and assigned a “pass” or “fail” rating.

Resolution

The results of the study concluded that a 1.0mm shaft clearance is generally sufficient for creating mechanical hinges. Conversely, it is not recommended to design hinges with only a 0.6mm clearance due to the fact that the knuckle will most likely fuse to the shaft, rendering it immobile.

Table 6: Hinge resolution at shaft clearances of 0.6 and 1.0mm for all test cubes. The values within each cell indicate the proportion of observed instances that correctly resolved.

Hinges	
Shaft Clearance (mm)	
1.0	0.6
0.85	0.22

Discussion

Consistent with the hole results, hinges built with the primary axis along the Z axis of the build chamber do not resolve as reliably. Also similar to previous features, the PA 12 hinges generally resolve much better than both GF PA 12 and FR PA 11. Hinges built in the exterior portion of the build chamber have slightly better resolution results than those built in the interior.

Lettering

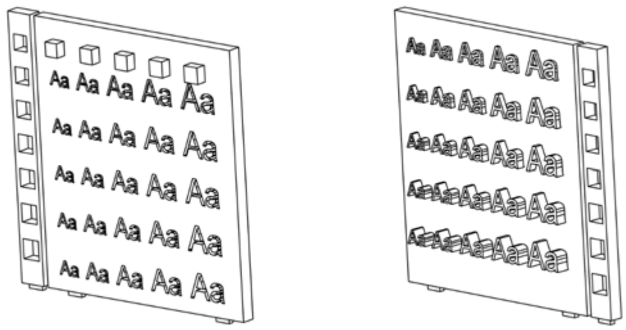

Figure 15: Lettering features for embossed (left) and extruded (right) letters

Many designers wish to include lettering on the surface of parts. Both embossed and raised lettering is tested at letter depths of 0.5mm to 2.5mm and font sizes ranging from 10pt to 18pt (Figure 15). The font is Arial (Regular), a sans-serif font. Both uppercase and lowercase forms of the letter “A” are used as the test font. Lettering resolution is determined by using the criteria outlined in Table 7.

Table 7: Convention used to evaluate lettering resolution

		
Pass	Intermediate	Fail

Resolution

Lettering resolution does not appear to depend significantly on the depth of the emboss/extrude, but depends substantially on the size of the font. Embossed lettering reliably resolved nearly all font sizes at all emboss depths. For this reason, a designer should consider embossed lettering as opposed to raised when adding text to a part that is additively manufactured using selective laser sintering. If raised lettering is desired, fonts larger than 16pt should be used.

Table 8: Resolution of embossed lettering for all test cubes

		Embossed Lettering				
		Font Size (pt)				
		10	12	14	16	18
Emboss Depth (mm)	0.5					
	1.0					
	1.5					
	2.0					
	2.5					

Table 9: Resolution of raised lettering for all test cubes

		Raised Lettering				
		Font Size (pt)				
		10	12	14	16	18
Extruded Depth (mm)	0.5					
	1.0					
	1.5					
	2.0					
	2.5					

Discussion

Lettering oriented along the Z axis of the build chamber performs worse than the other directions. This is due to the effects of spot size versus layer thickness mentioned in the thin walls section. Consistent with many of the other features, the best results are achieved with PA 12, followed by GF PA 12 then FR PA 11. Location within the build chamber does not produce a discernable effect on lettering resolution.

Snap Fits

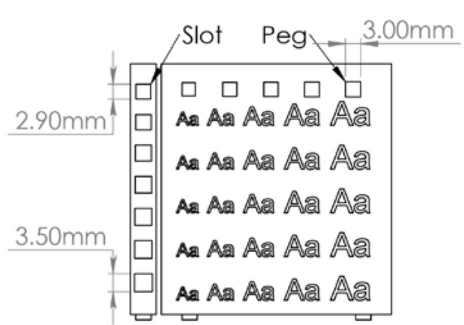

Figure 16: Snap fit features in the test part

The offset required for mechanical snap fits is determined by testing an extruded square peg against slots of varying size (Figure 16). Square pegs of 3.0mm nominal width are tested against slots of 2.9mm to 3.5mm nominal width in increments of 0.1mm. Snap fit resolution is then defined by the offset distance between the peg and slot that provides a snug fit.

Resolution

In general, when incorporating mechanical snap fits into a design, an offset of 0.15mm to 0.2mm should be used between the peg and slot. An example design and a depiction of the offset distance are shown in Figure 17.

Table 10: Snap fit resolution for all test cubes. Green boxes indicate the offsets that correspond to the best fit between the peg and slots. The values within each cell indicate the proportion of observed instances that correctly resolved.

Snap Fits						
Offset (mm)						
-0.05	0	0.05	0.1	0.15	0.2	0.25
0.09	0.07	0.1	0.13	0.26	0.23	0.12

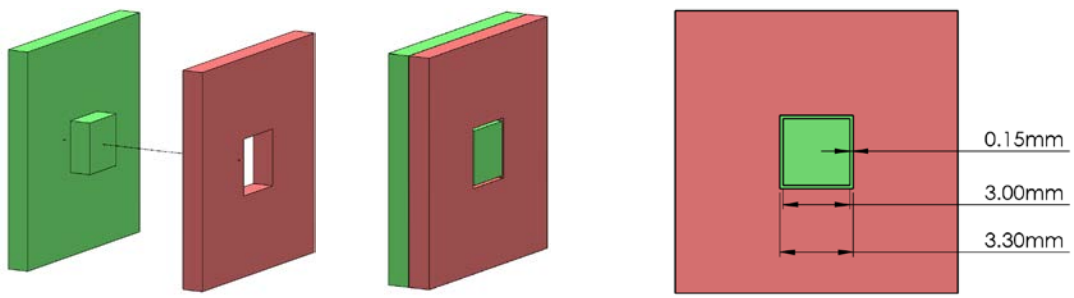

Figure 17: Example snap fit design. The image on the right shows an offset distance of 0.15mm between the peg and slot.

Discussion

Snap fits that are built with the primary axis orthogonal to the build chamber require a larger offset for the best performance compared with the other orientations. Attributed to the poorer resolution of the material, FR PA 11 snap fits require the largest offset compared with GF PA 12 and PA 12. The results do not suggest much dependence on location within the build chamber on snap fit design.

Analysis of Variance

An analysis of variance (ANOVA) test can be used to determine which factors in the metrology study are statistically significant. A follow-up multiple comparisons test describes the magnitude of the corresponding mean differences. Table 11 shows both the ANOVA and mean difference results from the polymer test cube measurement data. A separate analysis of variance is performed for each feature. The values in the table represent the percentage of features that found the given parameter to be statistically significant. First order interaction effects are also shown. The mean differences are presented as an average across all features and signify the average total variation attributed to each main effect. Due to manufacturing constraints, both the ANOVA and mean differences are calculated on a per-material basis for machine variation.

Table 11: Significant effects and mean differences.

	Significant Effects							
	M	O	L	M*O	M*L	O*L	Machine	Key
Percentage Significant	100%	60%	38%	27%	3%	7%	30%	M = Material O = Orientation L = Location * = Interaction Effect
Average Mean Difference (mm)	0.20	0.19	0.05	-	-	-	0.09	

Discussion

The test cube features can be broken down into two regimes: "additive" features and "subtractive" features. An "additive" feature is one in which the laser scans the feature geometry as in thin walls and rods. Gaps and holes are "subtractive" features in which the feature geometry is determined by voids in the laser scan area. The results indicate that "additive" features tend to be oversized compared to the nominal dimensions, while "subtractive" features tend to be undersized. The driving factor behind this phenomenon is oversintering. Oversintering occurs when the powder surrounding a part is unintentionally fused during the sintering process. The additional fused powder causes the dimensions of "additive" features to be larger than the as-designed values and "subtractive" features to be smaller. The oversintering effect appears to maintain a relatively constant value of 0.2mm for both feature regimes and does not appear to depend on feature size.

The results of the ANOVA test with multiple comparisons suggest that material and orientation are the most common statistically significant factors. The variation attributed to changing materials or orientations can lead to mean differences in dimensions as great as 0.4mm. Location within the build chamber is statistically significant for certain features, but the effect is generally minor with mean differences in dimensions around 0.05mm. Machine variation is also statistically significant for nearly one third of the features measured, but the effect appears to be relatively small. The online web tool contains much more detailed information on the effects of the various input parameters, including an interactive component that allows the user to filter the results for each parameter of interest.

Closure

In summary, process-specific test parts can be designed to characterize the different AM technologies. Compact and comprehensive test parts can be used in metrology studies to generate statistically significant results. The metrology study presented here investigates the effect of material, orientation within the build chamber, location within the build chamber, and machine identity for the polymer powder bed fusion process. The results are compiled into statistically-meaningful design guidelines and integrated into an online web tool. The web tool can be used by designers to reduce design iterations and aid in design decisions.

Future studies could be conducted to investigate new features or to build additional copies of the test part in order to increase the statistical fidelity of the results. The metrology strategy used for polymer PBF can also be applied to different AM process and added to the online web tool. The parts used in such studies should be process-specific so that the capabilities and limitations of each AM process are accurately captured.

Acknowledgements

This effort was performed through the National Center for Defense Manufacturing and Machining under the America Makes Program entitled “A Design Guidance System for Additive Manufacturing (Project 4053)” and is based on research sponsored by Air Force Research Laboratory under agreement number FA8650-12-2-7230. The U.S. Government is authorized to reproduce and distribute reprints for Governmental purpose notwithstanding any copyright notation thereon.

References

[1] M. Mahesh, Y.S. Wong, J.Y.T. Fug, H.T. Loh, "Benchmarking for comparative evaluation of RP systems and processes," *Rapid Prototyping Journal*, vol. 10, no. 2, pp. 123-135, 2004.

[2] L. Castillo, "Study about the rapid manufacturing of complex parts of stainless steel and titanium," TNO Industrial Technology, 2005.

[3] Shawn Moylan, John Slotwinski, April Cooke, Kevin Jurrens, M. Alkan Donmez, "An Additive Manufacturing Test Artifact," *Journal of Research of the National Institute of Standards and Technology*, vol. 119, pp. 429-459, 2014.

[4] Tyler Govett, Kevin Kim, Michael Lundin, Daniel Pinero, "Design Rules for Selective Laser Sintering," in *SFF Symposium*, Austin, TX, 2012.

[5] Wegner, A., Witt, G., "Correlation of process parameters and part properties in laser sintering using response surface modeling," *Physics Procedia*, vol. 39, pp. 480-490, 2012.

[6] Adam, G., Zimmer, D., "Design for Additive Manufacturing - Element transitions and aggregated structures," *CIRP Journal of Manufacturing Science and Technology*, vol. 7, pp. 20-28, 2014.

[7] J. Allison, C. Sharpe, C. Seepersad, "A Test Part for Evaluating the Accuracy and Resolution of a Polymer Powder Bed," *Journal of Mechanical Design*, 2017. In Press.

[8] Ian Gibson, Shi Dongping, "Material properties and fabrication parameters in selective laser sintering process," *Rapid Prototyping Journal*, vol. 3, no. 4, pp. 129-135, 1997.

[9] David L Bourell, Ming C. Leu, David W. Rosen, "Roadmap for Additive Manufacturing," Washington D.C., 2009.

[10] J.P. Kruth, X. Wang, T. Laoui, L. Froyen, "Lasers and materials in selective laser sintering," *Assembly Automation*, vol. 23, no. 4, pp. 357-371, 2003.

[11] U. Ajoku, N. Saleh, N. Hopkinson, R. Hague, P. Erasenthiran, "Investigating mechanical anisotropy and end-of-vector effect in laser-sintered nylon parts," vol. 220, no. 7, pp. 1077-1086, 2006.

[12] Cooke, W., Tomlinson, R.A., Burguete, R., Johns, D., Vanard, G., "Anisotropy, homogeneity and ageing in an SLS polymer," *Rapid Prototyping Journal*, vol. 17, no. 4, pp. 269-279, 2011.

[13] B. Caulfield, P.E. McHugh, S. Lohfeld, "Dependence of mechanical properties of polyamide componenets on build parameters in the SLS process," *Journal of Materials Processing Technology*, vol. 182, pp. 477-488, 2007.

[14] David L. Bourell, Trevor J. Watt, David K. Leigh, Ben Fulcher, "Performance limitations in polymer laser sintering," vol. 56, pp. 147-156, 2014.